

## Supporting Information

# Interplaying anions in a supramolecular metallohydrogel to form metal organic frameworks

Suwendu Karak,<sup>a,b,‡</sup> Sushil Kumar,<sup>a,‡</sup> Saibal Bera,<sup>a,b</sup> David Díaz Díaz<sup>c,d</sup> Subhrashis Banerjee,<sup>a,b</sup> Kumar Vanka<sup>a,b</sup> and Rahul Banerjee<sup>\*a,b</sup>

*Physical/Materials Chemistry Division, CSIR-National Chemical Laboratory, Dr. Homi Bhabha Road,  
Pune 411 008, India. Email: [r.banerjee@ncl.res.in](mailto:r.banerjee@ncl.res.in)*

*Academy of Scientific and Innovative Research (AcSIR), New Delhi, India  
Universität Regensburg, Universitätsstrasse 31, 93053 Regensburg, Germany.  
Institute of Advanced Chemistry of Catalonia (IQAC-CSIC), Spain.*

## Contents

	Page
1. Materials	S3
2. Physical Measurements	S3
3. Crystallography	S3
4. Synthesis of H <sub>2</sub> L ligand (IL)	S3
5. Synthesis of ZAIL	S4
6. General procedure for synthesis of ZAIL-X	S4
7. The anion effect on gel synthesis	S7
8. Crystallographic details of the as synthesized MOFs	S15
9. Computational details	S21
10. References	S28

## 1. Materials

All materials were used as received. Acetonitrile was dried and distilled by refluxing over  $\text{CaH}_2$  and stored over 4 Å molecular sieves. Methylene chloride was dried and distilled over  $\text{CaCl}_2$  and stored over 4 Å molecular sieves.

## 2. Physical Measurements

Fourier Transform Infra Red spectroscopy was recorded on a Bruker Optics Alpha E Spectrometer with a universal Zn-Se-ATR (Attenuated Total Reflection) accessory in the 600 - 4000  $\text{cm}^{-1}$  region or using a Diamond ATR (Golden Gate). SEM images were obtained with a Zeiss DSM 950 scanning electron microscope and FEI, QUANTA 200 3D Scanning Electron Microscope with tungsten filament as electron source operated at 10 kV. The samples were sputtered with Au (nano sized film) prior to imaging by a SCD 040 Balzers Union. TEM images were recorded using FEI Tecnai G2 F20 X-TWIN TEM at an accelerating voltage of 200 kV. The TEM Samples were prepared by drop casting the sample dispersed in isopropanol or water and direct layer coating on copper grids TEM Window (TED PELLA, INC. 200 mesh). NMR data were taken in Bruker 200 MHz NMR spectrometer. Optical images of samples were taken by Modular Routine Stereo Microscope with 8:1 Zoom Leica M80.

## 3. Crystallography

Powder X-Ray Diffraction patterns were performed on a Rigaku, Micromax-007HF with high intensity micro focus rotating anode X-Ray generator. The X-ray diffraction data were collected on an Oxford CCD diffractometer equipped with an Supernova (Mo) X-Ray diffraction measurement device using graphite-monochromated  $\text{Mo-K}_\alpha$  radiation ( $\lambda = 0.71073$  Å).<sup>2</sup> Multi-scan absorption correction was also applied.<sup>2</sup> The structures were solved by the direct method using SIR-92<sup>3</sup> and refined by full matrix least-square refinement techniques on  $F^2$  using SHELXL-2016/4.<sup>4</sup> All calculations were carried out with the WinGx crystallographic package.<sup>5</sup> The non-hydrogen atoms were anisotropically refined whereas the hydrogen atoms were placed into the calculated positions and included in the last cycles of the refinement. For ZAIL-Br,

ZAIL-N3 MOFs we have tried several crystals from couple of batches for the best one. However, due to poor quality of the crystal it has shown  $R_{\text{int}}$  value of 0.15 and 0.16, respectively and thus has generated the Alert level B and Alert level C, respectively, in checkcif. In case of ZAIL-OAc, there is one water molecule (from electron density map) present in the lattice of unit cell. However, due to presence of disorder in the oxygen atom we were unable to assign hydrogen to this oxygen atom precisely and thus are reporting as it is. This has generated Alert level B in check cif.

#### **4. Synthesis of H<sub>2</sub>L ligand (IL)**

The ligand IL was prepared following reported the procedure previously reported in the literature.<sup>1</sup> To an aqueous solution (20 mL) of L-isoleucine (0.5 g, 3.81 mmol) and Na<sub>2</sub>CO<sub>3</sub> (1.0 g, 9.52 mmol), 4-pyridinecarboxaldehyde (0.408 g, 3.81 mmol) was added slowly. The solution was stirred for 3 h at 60 °C. The mixture was spontaneously cooled to room temperature and then subjected to ice-bath. NaBH<sub>4</sub> was added slowly to the reaction mixture at 0 °C and stirred for 12 h. Acetic acid solution (6M) was then added to neutralize the excess of sodium carbonate until pH 7.2-7.5. The reaction mixture was further stirred for 1h. The aqueous solution was washed with methylene chloride (3 x 25 mL). The water was subsequently removed under reduced pressure. Acetonitrile (40 mL) was added to the resulting crude white precipitate and the mixture was sonicated for 1 h. The obtained white product was then filtered and dried under vacuum. Yield: 0.83 g (98.15 %). <sup>1</sup>H NMR (200 MHz, D<sub>2</sub>O) δ 8.52 (d, *J* = 6.2 Hz, 2H), 7.45 (d, *J* = 6.2 Hz, 2H), 4.33 – 4.10 (m, 2H), 3.45 (d, *J* = 3.8 Hz, 1H), 1.99 – 1.72 (m, 1H), 1.53 – 1.32 (m, 1H), 1.30 – 1.10 (m, 1H), 0.82 (dd, *J* = 14.5, 7.1 Hz, 6H). <sup>13</sup>C NMR (101 MHz, D<sub>2</sub>O) δ 172.17 (C6), 149.40 (C1), 140.80 (C3), 125.19 (C2), 66.58 (C5), 49.50 (C4), 35.94 (C7), 25.74 (C8), 14.19 (C10), 11.04 (C9).

#### **5. Synthesis of ZAIL**

0.5 mL of aqueous solution of zinc acetate (0.082 g, 0.450 mmol) was mixed with 0.5 mL aqueous of solution of ligand (0.2 g, 0.90 mmol) in a test tube followed by sonication affording the immediate formation of ZAIL.

#### **6. General procedure for synthesis of ZAIL-X (Method A)**

0.5 mL aqueous solution of NaX salt (X = Cl, Br, N<sub>3</sub>, NO<sub>3</sub>, OTs, OAc) was layered on top of ZAIL (obtained from 0.2 g of ligand) and left undisturbed for 2-3 days. Gradual degradation of the gel over time was accompanied by concomitant formation of the corresponding ZAIL-X metal organic framework.

**Method B.** 0.2 g of NaX salt (X = Cl, Br, N<sub>3</sub>, NO<sub>3</sub>, OTs, OAc) was sprinkled over the top of ZAIL (obtained from 0.2 g of ligand) and left undisturbed for 2-3 days. Gradual degradation of the gel over time was accompanied by concomitant formation of the corresponding ZAIL-X metal organic framework.

**ZAIL-Cl.** Yield 0.23 g (75.81 %). FTIR 3158 ( $\nu_{\text{N-H}}$ ), 2968, 2928, 2905, 2873 ( $\nu_{\text{C-H}}$ ), 1630 ( $\nu_{\text{C=O}}$ ), 1558, 1475, 1452, 1434 ( $\nu_{\text{C=C}}$ ), 1385, 1336, 769, 734 ( $\nu_{\text{C-H bending}}$ )  $\text{cm}^{-1}$ .

**ZAIL-Br.** Yield 0.26 g (75.69 %). FTIR (Zn-Se ATR): 3160 ( $\nu_{\text{N-H}}$ ), 2965, 2914, 2870 ( $\nu_{\text{C-H}}$ ), 1632 ( $\nu_{\text{C=O}}$ ), 1620, 1476, 1448, 1434, 1482 ( $\nu_{\text{C=C}}$ ), 1435, 1031, 761, 732 ( $\nu_{\text{C-H bending}}$ )  $\text{cm}^{-1}$ .

**ZAIL-N<sub>3</sub>.** Yield 0.22 g (67.74 %). FTIR (Zn-Se ATR): 3252 ( $\nu_{\text{N-H}}$ ), 2950, 2903, 2870 ( $\nu_{\text{C-H}}$ ), 2062, 1593 ( $\nu_{\text{C=O}}$ ), 1556, 1430 ( $\nu_{\text{C=C}}$ ), 1338, 1069, 754 ( $\nu_{\text{C-H bending}}$ )  $\text{cm}^{-1}$ .

**ZAIL-OAc.** Yield 0.24 g (73.84%). FTIR (Zn-Se ATR): 3156 ( $\nu_{\text{N-H}}$ ), 2966, 2918, 2859 ( $\nu_{\text{C-H}}$ ), 1632 ( $\nu_{\text{C=O}}$ ), 1563, 1478 ( $\nu_{\text{C=C}}$ ), 1431, 1387, 1068, 753 ( $\nu_{\text{C-H bending}}$ )  $\text{cm}^{-1}$ .

**ZAIL-NO<sub>3</sub>.** Yield 0.24 g (74.69 %). FTIR (Zn-Se ATR): 3187 ( $\nu_{\text{N-H}}$ ), 2966, 2936, 2875 ( $\nu_{\text{C-H}}$ ), 1623 ( $\nu_{\text{C=O}}$ ), 1569, 1489 ( $\nu_{\text{C=C}}$ ), 1432, 1385, 1024, 752 ( $\nu_{\text{C-H bending}}$ )  $\text{cm}^{-1}$ .

**ZAIL-OTs.** Yield 0.32 g (77.91%). FTIR (Zn-Se ATR): 1626, 1562, 1421, 1025, 806, 686  $\text{cm}^{-1}$ .

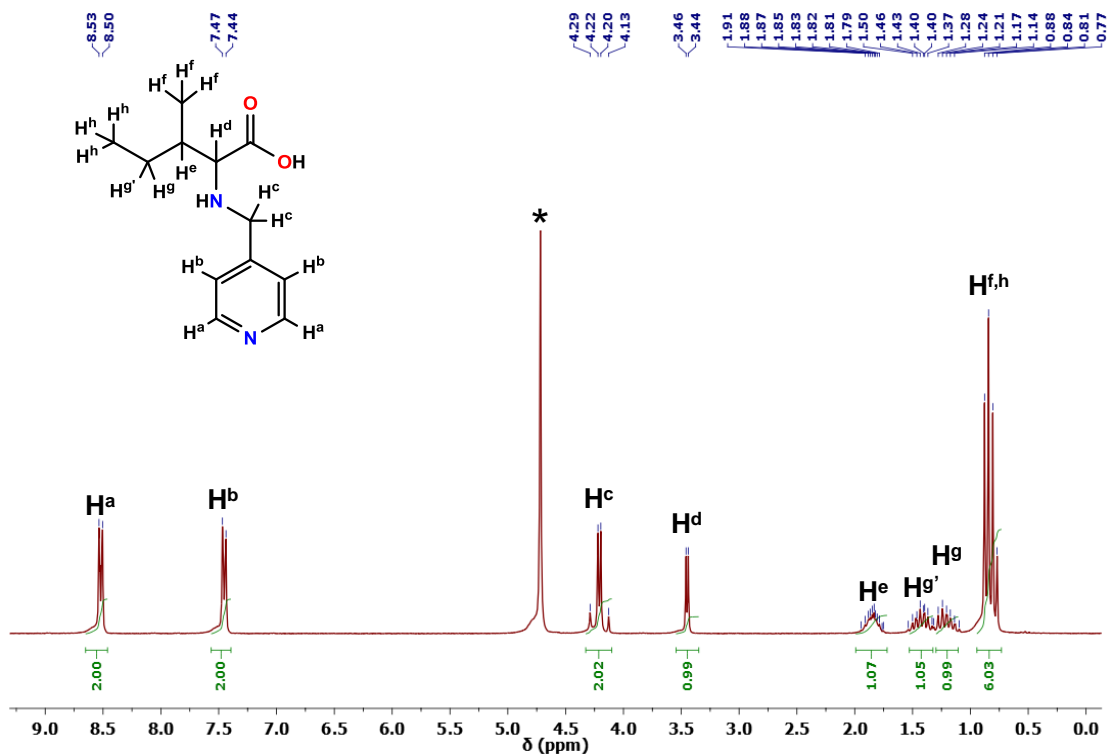


**Fig. S1** <sup>1</sup>H NMR spectrum of IL recorded in D<sub>2</sub>O whereas asterisk represents residual solvent peak.

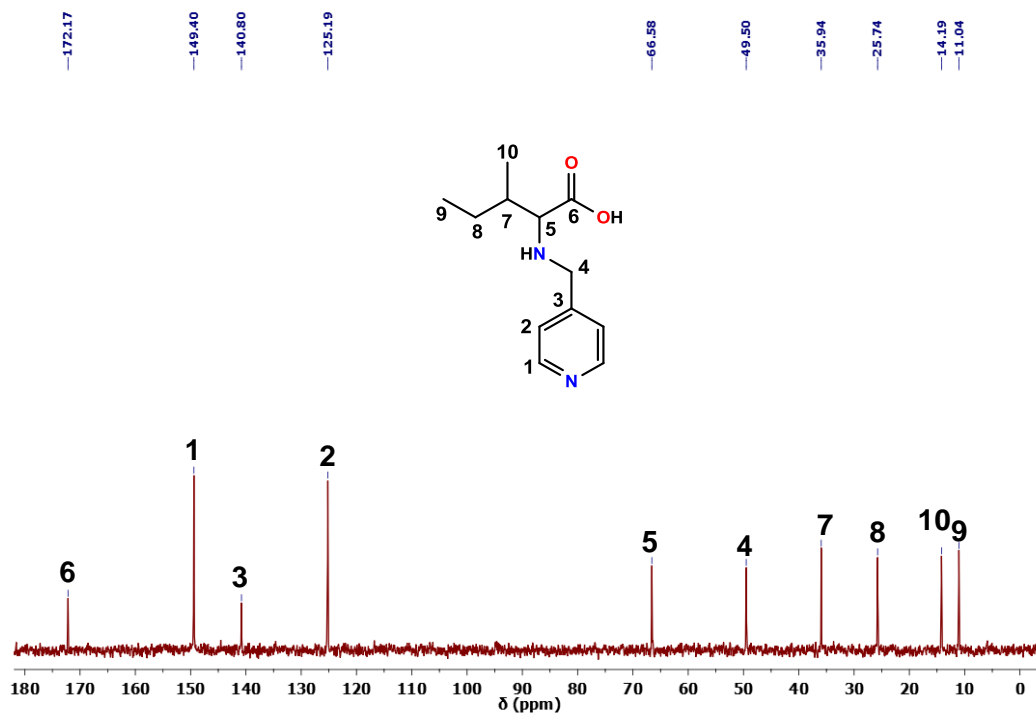


**Fig. S2** <sup>13</sup>C NMR spectrum of IL recorded in D<sub>2</sub>O.

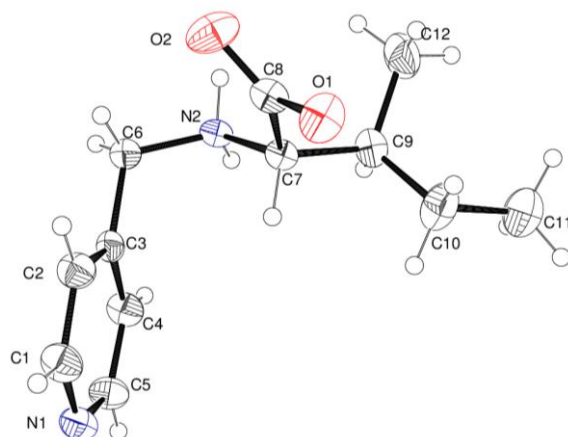


**Fig. S3** Molecular structure of IL whereas thermal ellipsoids are drawn at 50 % probability level.

### 7. The anion effect on gel synthesis

The anions play the crucial role in connecting the gelator with each other through hydrogen bonding. Finally, the aggregation of the gelator fibril results in the formation of the gel matrix. Nitrate and acetate ion direct multiple hydrogen bonding which result in the formation of this cross-linking within the gel matrix. As there is hydrophobic part in the gelator, cross-linking requires strong hydrogen bonding with water as well as with the anions. In case of perchlorate and tetrafluoroborate ion, the charge is more diffused which results in weaker hydrogen bonding. Thus, weak hydrogen bonding and poor cross-linking make chloride, bromide, perchlorate, tosylate and tetrafluoroborate ions inefficient for the formation of gel matrix.

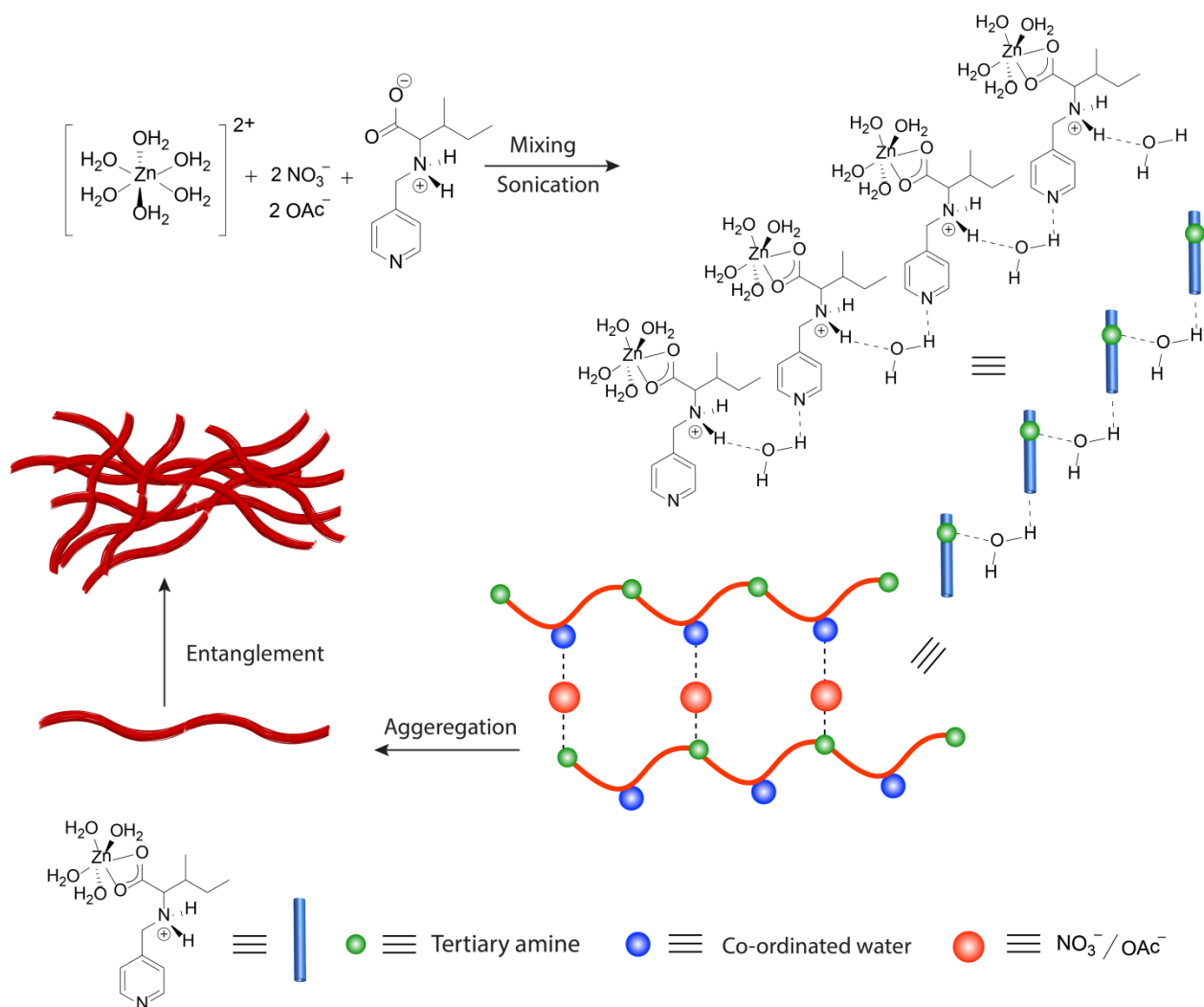


**Fig. S4** Plausible mechanism of formation of the gelator complex and subsequent formation of supramolecular aggregate.

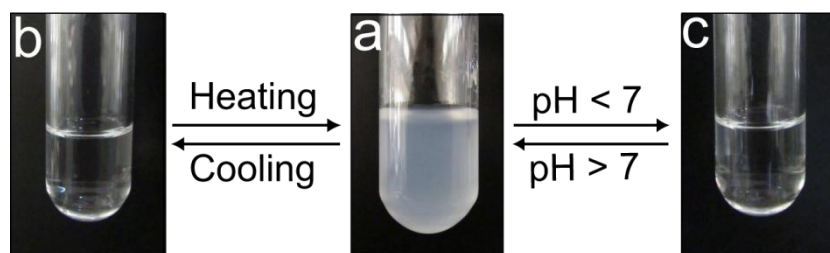


**Fig. S5** pH and temperature dependent reversible behavior of ZAIL.

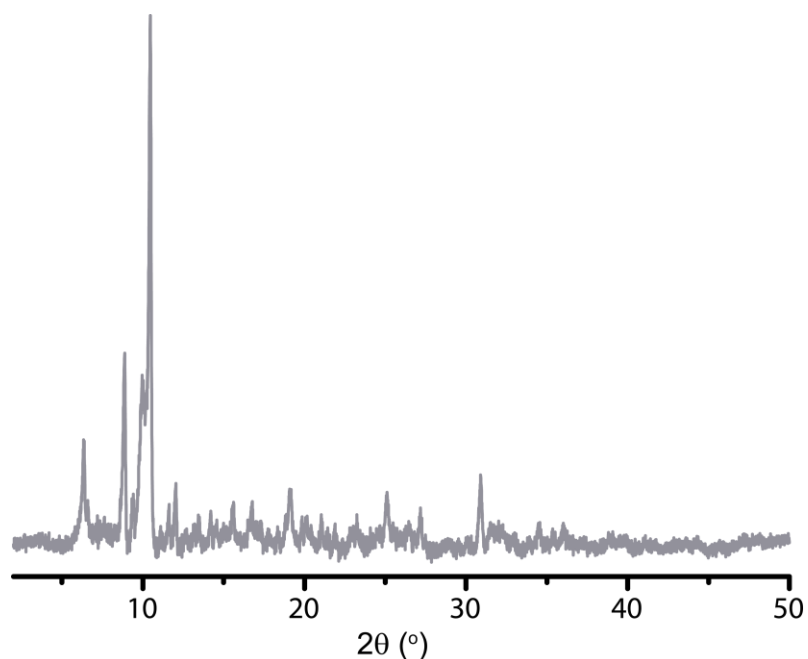


**Fig. S6** PXRD pattern of ZAIL recorded in its xerogel state.

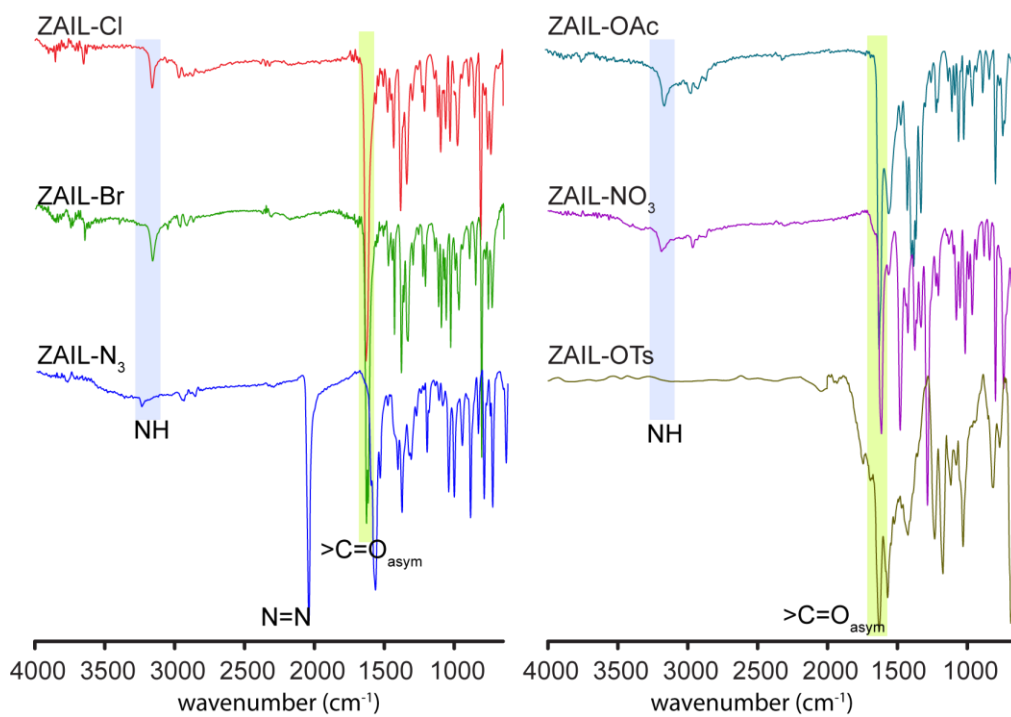


**Fig. S7** FTIR spectra of ZAIL-Cl, ZAIL-Br, ZAIL-N<sub>3</sub>, ZAIL-OAc, ZAIL-NO<sub>3</sub>, and ZAIL-OTs MOFs.

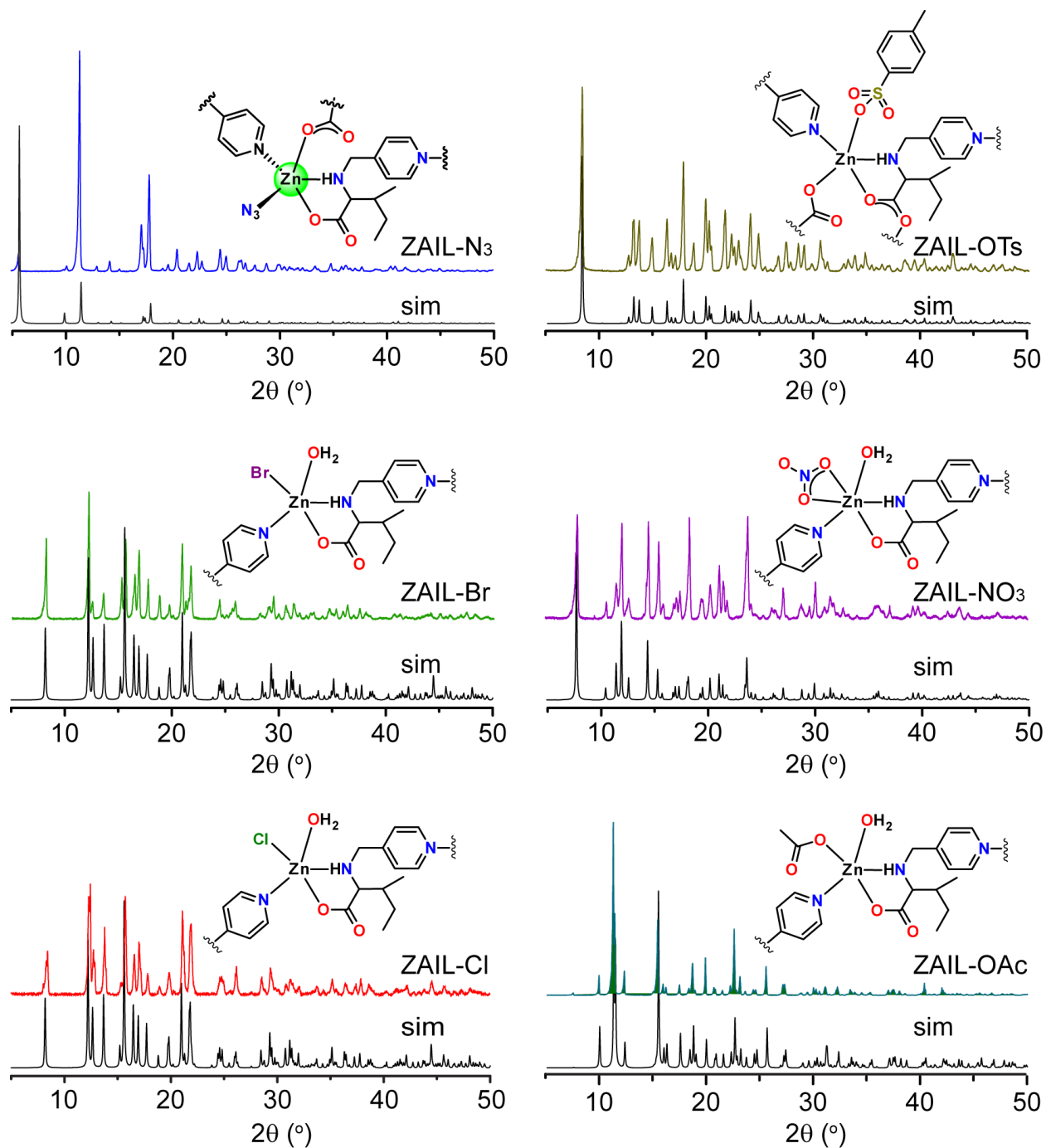


**Fig. S8** PXRD patterns of ZAIL-Cl, ZAIL-Br, ZAIL-N<sub>3</sub>, ZAIL-OAc-ZAIL-NO<sub>3</sub>, and ZAIL-OTs MOFs.

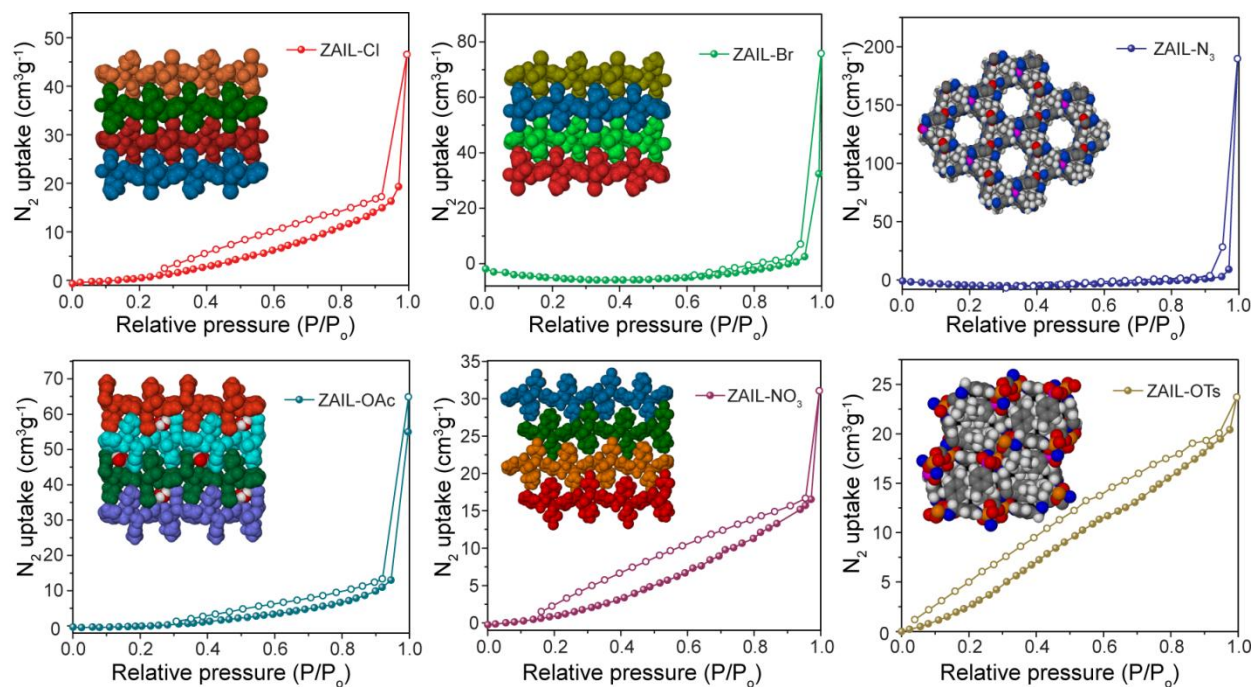


**Fig. S9**  $N_2$  gas adsorption of the as-synthesized MOFs.

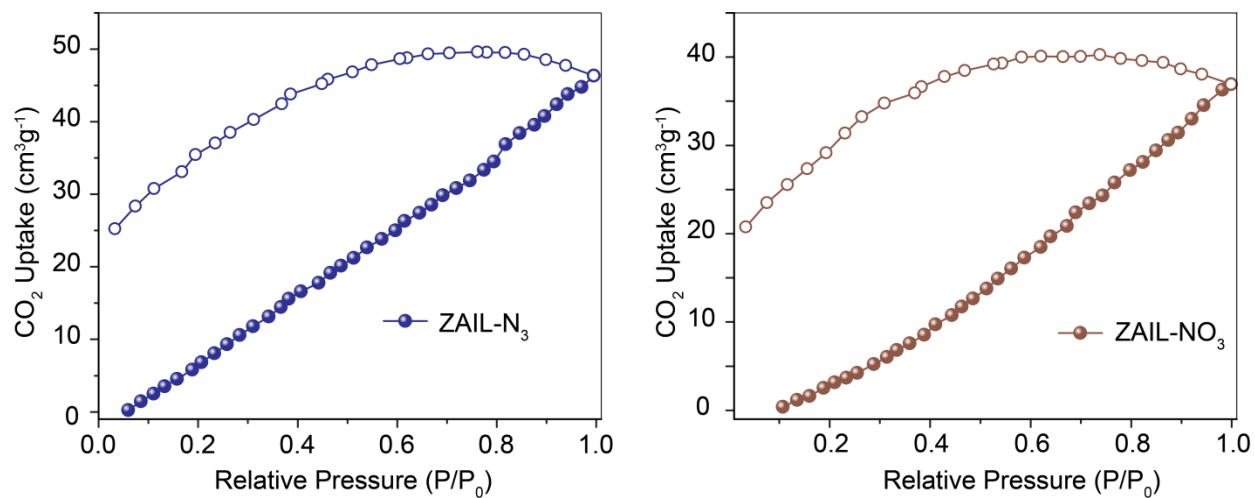


**Fig. S10**  $CO_2$  gas adsorption of the as-synthesized MOFs.

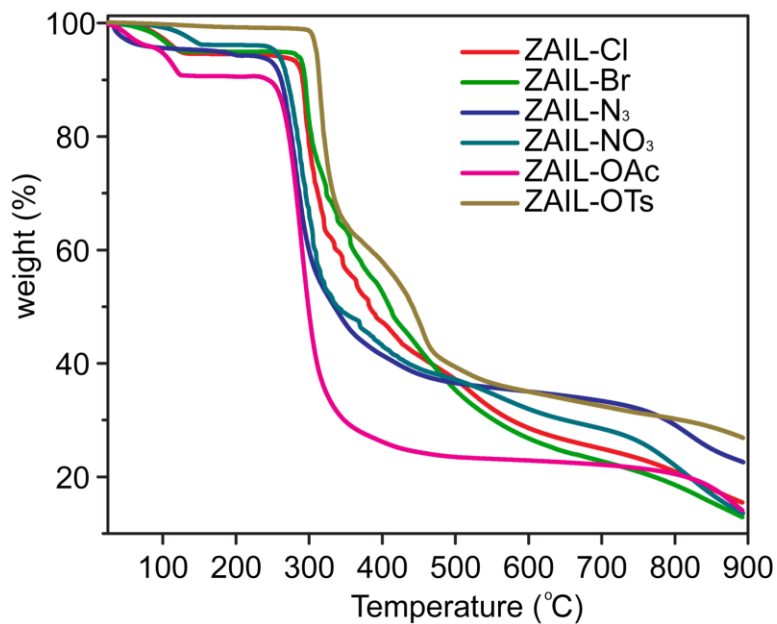


**Fig. S11** TGA studies done for ZAIL-Cl, ZAIL-Br, ZAIL-N<sub>3</sub>, ZAIL-OAc, ZAIL-NO<sub>3</sub>, and ZAIL-OTs MOFs.

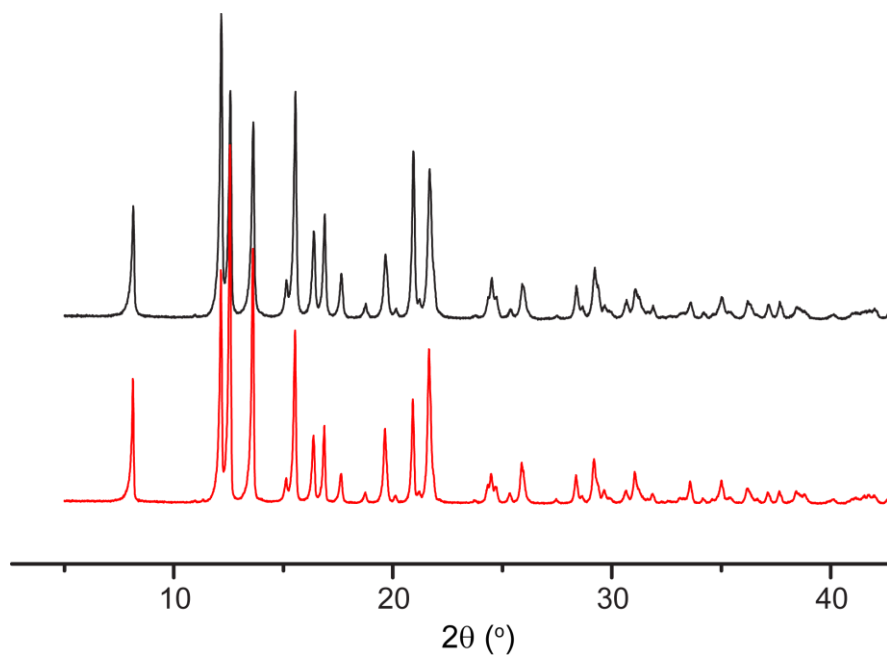


**Fig. S12** PXRD patterns for ZAIL-Cl obtained via layering method A (Red) and method B (black).

**Table S1.** Microanalysis of all the as-synthesized MOFs<sup>a</sup>.

MOFs	% C	% N	% H
ZAIL-Cl	42.02 (42.38)	5.52 (5.63)	8.10 (8.24)
ZAIL-Br	37.85 (37.48)	5.37 (4.98)	7.10 (7.28)
ZAIL-OAc	46.46 (46.23)	6.11 (6.10)	7.63 (7.70)
ZAIL-N <sub>3</sub>	44.20 (43.85)	5.50 (5.21)	21.00 (21.31)
ZAIL-NO <sub>3</sub>	39.71 (39.31)	5.20 (5.22)	11.34 (11.46)
ZAIL-OTs	49.17 (49.73)	5.60 (5.49)	6.69 (6.11)

<sup>a</sup>Value in parenthesis indicate the calculated values.

**Table S2.** Crystallographic structural parameters of ZAIL-Cl, ZAIL-Br, ZAIL-N<sub>3</sub>, ZAIL-OAc-ZAIL-NO<sub>3</sub>, and ZAIL-OTs MOFs.

	H <sub>2</sub> L	ZAIL-Cl	ZAIL-Br	ZAIL-N <sub>3</sub>	ZAIL-NO <sub>3</sub>	ZAIL-OAc	ZAIL-OTs
Empirical formula	C <sub>12</sub> H <sub>18</sub> N <sub>2</sub> O <sub>2</sub>	C <sub>12</sub> H <sub>19</sub> N <sub>2</sub> O <sub>3</sub> ClZn	C <sub>12</sub> H <sub>19</sub> BrN <sub>2</sub> O <sub>3</sub> Zn	C <sub>12</sub> H <sub>17</sub> N <sub>3</sub> O <sub>2</sub> Zn	C <sub>12</sub> H <sub>19</sub> N <sub>3</sub> O <sub>6</sub> Zn	C <sub>14</sub> H <sub>22</sub> N <sub>2</sub> O <sub>6</sub> Zn	C <sub>19</sub> H <sub>22</sub> N <sub>2</sub> O <sub>5</sub> SZn
Formula weight	222.28	340.11	384.57	328.68	366.67	379.70	455.81
Temperature	293(2) K	293(2) K	293(2) K	293(2) K	293(2) K	293(2) K	293(2) K
Wavelength	0.71073 Å	0.71073 Å	0.71073 Å	0.71073 Å	0.71073 Å	0.71073 Å	1.54184 Å
Crystal system	Monoclinic	orthorhombic	orthorhombic	Hexagonal	Monoclinic	orthorhombic	orthorhombic
Space group	<i>P</i> 2 <sub>1</sub>	<i>P</i> 2 <sub>1</sub> 2 <sub>1</sub> 2 <sub>1</sub>	<i>P</i> 2 <sub>1</sub> 2 <sub>1</sub> 2 <sub>1</sub>	<i>P</i> 6 <sub>1</sub>	<i>P</i> 2 <sub>1</sub>	<i>P</i> 2 <sub>1</sub> 2 <sub>1</sub> 2 <sub>1</sub>	<i>P</i> 2 <sub>1</sub> 2 <sub>1</sub> 2 <sub>1</sub>
<i>a</i>	7.7667(3) Å	6.2031(2) Å	6.2078(6) Å	17.764(3) Å	6.1863(3) Å	6.166(5) Å	8.2326(2) Å
<i>b</i>	5.8151(2) Å	13.9957(6) Å	14.2553(11) Å	17.764(3) Å	16.8458(7) Å	15.763(5) Å	13.5545(3) Å
<i>c</i>	13.6758(6) Å	16.9125(6) Å	17.0701(16) Å	10.4098(12) Å	15.5108(13) Å	17.831(5) Å	17.4759(4) Å
$\alpha$	90°	90°	90°	90°	90°	90.0 (5)°	90°
$\beta$	102.312(4)°	90°	90°	90°	96.948(6)°	90.0 (5)°	90°
$\gamma$	90°	90°	90°	120°	90°	90.0 (5)°	90°
Volume	603.45(4) Å <sup>3</sup>	1468.29(9) Å <sup>3</sup>	1510.6(2) Å <sup>3</sup>	2844.7(9) Å <sup>3</sup>	1604.56(17) Å <sup>3</sup>	1733.1(16) Å <sup>3</sup>	1950.11(8) Å <sup>3</sup>
Z	2	4	4	6	4	4	4
Density (calculated)	1.223 Mg/m <sup>3</sup>	1.539 Mg/m <sup>3</sup>	1.691 Mg/m <sup>3</sup>	1.151 Mg/m <sup>3</sup>	1.518 Mg/m <sup>3</sup>	1.455 Mg/m <sup>3</sup>	1.553 Mg/m <sup>3</sup>
Absorption coefficient	0.084 mm <sup>-1</sup>	1.859 mm <sup>-1</sup>	4.276 mm <sup>-1</sup>	1.302 mm <sup>-1</sup>	1.561 mm <sup>-1</sup>	1.447 mm <sup>-1</sup>	3.046 mm <sup>-1</sup>
<i>F</i> (000)	240	704	776	1020	760	792	944
Crystal size	0.230 x 0.200 x 0.180 mm <sup>3</sup>	0.25 x 0.20 x 0.18 mm <sup>3</sup>	0.240 x 0.220 x 0.180 mm <sup>3</sup>	0.260 x 0.220 x 0.190 mm <sup>3</sup>	0.260 x 0.250 x 0.180 mm <sup>3</sup>	0.260 x 0.220 x 0.200 mm <sup>3</sup>	0.24 x 0.21 x 0.19 mm <sup>3</sup>
Theta range for data collection	3.049 to 24.993°	3.150 to 24.997°	3.097 to 24.981°	3.015 to 24.996°	2.909 to 24.995°	3.450 to 24.998°	5.941 to 67.985°
Index ranges	-9 ≤ <i>h</i> ≤ 7, -6 ≤ <i>k</i> ≤ 4, -13 ≤ <i>l</i> ≤ 16	-4 ≤ <i>h</i> ≤ 7, -13 ≤ <i>k</i> ≤ 16, -20 ≤ <i>l</i> ≤ 18	-7 ≤ <i>h</i> ≤ 3, -8 ≤ <i>k</i> ≤ 16, 20 ≤ <i>l</i> ≤ 19	-17 ≤ <i>h</i> ≤ 21, -20 ≤ <i>k</i> ≤ 20, 12 ≤ <i>l</i> ≤ 8	-7 ≤ <i>h</i> ≤ 5, -20 ≤ <i>k</i> ≤ 20, 14 ≤ <i>l</i> ≤ 18	-7 ≤ <i>h</i> ≤ 6, -13 ≤ <i>k</i> ≤ 18, 20 ≤ <i>l</i> ≤ 21	-9 ≤ <i>h</i> ≤ 9, -12 ≤ <i>k</i> ≤ 16, -18 ≤ <i>l</i> ≤ 20
Reflections collected	2231	3440	3427	7358	5942	4137	4663
Independent reflections	1573 [ <i>R</i> (int) = 0.0201]	2306 [ <i>R</i> (int) = 0.0343]	2238 [ <i>R</i> (int) = 0.1499]	2732 [ <i>R</i> (int) = 0.1607]	4482 [ <i>R</i> (int) = 0.0692]	2861 [ <i>R</i> (int) = 0.0549]	3087 [ <i>R</i> (int) = 0.0191]
Completeness to theta = 25.00°	99.7 %	99.5 %	98.5 %	99.8 %	99.8 %	99.7 %	94.1 %
Absorption correction	Multi-scan	Multi-scan	Multi-scan	Multi-scan	Multi-scan	Multi-scan	Multi-scan
Max. and min. transmission	0.985 and 0.981	0.716 and 0.646	0.463 and 0.373	0.781 and 0.720	0.755 and 0.673	0.749 and 0.693	0.561 and 0.505
Refinement method	Full-matrix least-squares on <i>F</i> <sup>2</sup>	Full-matrix least-squares on <i>F</i> <sup>2</sup>	Full-matrix least-squares on <i>F</i> <sup>2</sup>	Full-matrix least-squares on <i>F</i> <sup>2</sup>	Full-matrix least-squares on <i>F</i> <sup>2</sup>	Full-matrix least-squares on <i>F</i> <sup>2</sup>	Full-matrix least-squares on <i>F</i> <sup>2</sup>
Data / restraints / parameters	1573 / 1 / 147	2306 / 5 / 192	2238 / 0 / 175	2732 / 1 / 183	4482 / 1 / 403	2861 / 0 / 212	3087 / 1 / 265
Goodness-of-fit on <i>F</i> <sup>2</sup>	1.164	0.928	0.962	1.013	1.027	1.054	1.088
Final <i>R</i> indices	<i>R</i> <sub>1</sub> = 0.0393, <i>wR</i> <sub>2</sub> = 0.0991	<i>R</i> <sub>1</sub> = 0.0337, <i>wR</i> <sub>2</sub> = 0.0509	<i>R</i> <sub>1</sub> = 0.0997, <i>wR</i> <sub>2</sub> = 0.2160	<i>R</i> <sub>1</sub> = 0.0864, <i>wR</i> <sub>2</sub> = 0.2175	<i>R</i> <sub>1</sub> = 0.0705, <i>wR</i> <sub>2</sub> = 0.1838	<i>R</i> <sub>1</sub> = 0.0594, <i>wR</i> <sub>2</sub> = 0.1667	<i>R</i> <sub>1</sub> = 0.0402, <i>wR</i> <sub>2</sub> = 0.1122
[ <i>I</i> > 2σ( <i>I</i> )] <sup>a, b</sup>	<i>R</i> <sub>1</sub> = 0.0417, <i>wR</i> <sub>2</sub> = 0.1003	<i>R</i> <sub>1</sub> = 0.0446, <i>wR</i> <sub>2</sub> = 0.0533	<i>R</i> <sub>1</sub> = 0.1519, <i>wR</i> <sub>2</sub> = 0.2708	<i>R</i> <sub>1</sub> = 0.1268, <i>wR</i> <sub>2</sub> = 0.2485	<i>R</i> <sub>1</sub> = 0.0800, <i>wR</i> <sub>2</sub> = 0.1949	<i>R</i> <sub>1</sub> = 0.0622, <i>wR</i> <sub>2</sub> = 0.1715	<i>R</i> <sub>1</sub> = 0.0417, <i>wR</i> <sub>2</sub> = 0.1186
Largest diff. peak and hole	0.128 and -0.139 e.Å <sup>-3</sup>	0.285 and -0.267 e.Å <sup>-3</sup>	0.897 and -1.095 e.Å <sup>-3</sup>	0.608 and -0.460 e.Å <sup>-3</sup>	0.606 and -1.087 e.Å <sup>-3</sup>	0.612 and -0.715 e.Å <sup>-3</sup>	1.166 and -0.519 e.Å <sup>-3</sup>

## 8. Crystallographic details of the as synthesized MOFs

ZAIL-X MOFs (X= Cl, Br, OTs, OAc, N<sub>3</sub> and NO<sub>3</sub>) discussed herein were synthesized by layering the gel both with solid salt and its aqueous solution. Crystals suitable for single-crystal X-ray diffraction studies were grown in 6 - 12 h. ZAIL-Cl, ZAIL-Br, ZAIL-OAc, and ZAIL-NO<sub>3</sub> (nitrate ion is coordinated to zinc ion in its bidentate form) are structural isomers with different anions coordinated to the zinc metal ion concerning ligand framework. Interestingly, ZAIL-Cl, ZAIL-Br and ZAIL-OAc crystallize in the P212121 space group where ZAIL-NO<sub>3</sub> in a P21 space group, respectively. In general, the geometry around the Zn(II) ion, among all MOFs reported in this manuscript, is either a distorted trigonal bipyramidal or a distorted square-pyramidal. For example, in the representative molecular structure of ZAIL-Cl, the Zn(II) center adopts a distorted trigonal bipyramidal geometry ( $\tau = 0.725$ ), chelated by protonated N<sub>amine</sub> (Zn1-N1: 2.093(4) Å) and introduced chloride anion (Zn1-Cl1: 2.225(1) Å). The third equatorial coordination was served by one pyridyl functionality of second IL ligand (Zn1-N2: 2.056(3) Å). In conjunction, all three coordination sites including zinc ion thus constitute an N<sub>2</sub>Cl basal plane. Apart from this, the axial coordination sites were occupied by monodentate carboxylate (Zn1-O1: 2.160(4) Å) of the first IL ligand and one O<sub>water</sub> molecule (Zn1-O2: 2.136(4) Å). For ZAIL-N<sub>3</sub>, the equatorial basal plane is consist of zinc ion coordinated to the ligand backbone via N<sub>amine</sub> (Zn1-N1: 2.084(10) Å), N'<sub>pyridine</sub> (Zn1-N2: 2.030(12) Å), and N<sub>azide</sub> (Zn1-N3: 1.972(15) Å) atoms. In addition, the axial sites were served by bridging carboxylate functionality i.e. O<sub>carboxylate</sub> (Zn1-O1: (2.138(10) Å) from the same ligand and O'<sub>carboxylate</sub> (Zn1-O2: 2.098(12) Å) from the second ligand. As aforementioned, the ZAIL-OTs adopts a distorted square-pyramidal geometry ( $\tau = 0.421$ ). The zinc ion is coordinated to O<sub>carboxylate</sub> (Zn1-O1: 2.070(4) Å), N<sub>amine</sub> (Zn1-N2: 2.102(5) Å), O<sub>tosylate</sub> (Zn1-O3: 2.154(4) Å), and O<sub>carboxylate</sub> (Zn1-O2: 1.962(4) Å), thus forms an NO<sub>2</sub>X plane. The axial coordination is served by N<sub>pyridine</sub> (Zn1-N1: 2.089(5) Å).

ZAIL-Cl, ZAIL-Br, ZAIL-OAc, and ZAIL-NO<sub>3</sub> MOFs form one-dimensional chains (view along crystallographic b-axis). These 1D chains were further connected to each other through weak hydrogen bonding interactions exist between O<sub>carboxylate</sub> and water protons; and O<sub>carboxylate</sub> and NH<sub>amine</sub>' respectively. On the other hand, for ZAIL-N<sub>3</sub> and ZAIL-OTs MOFs, the presence of bridging carboxylate functionality consequence in the formation of a three-dimensional network (view along crystallographic c-axis).

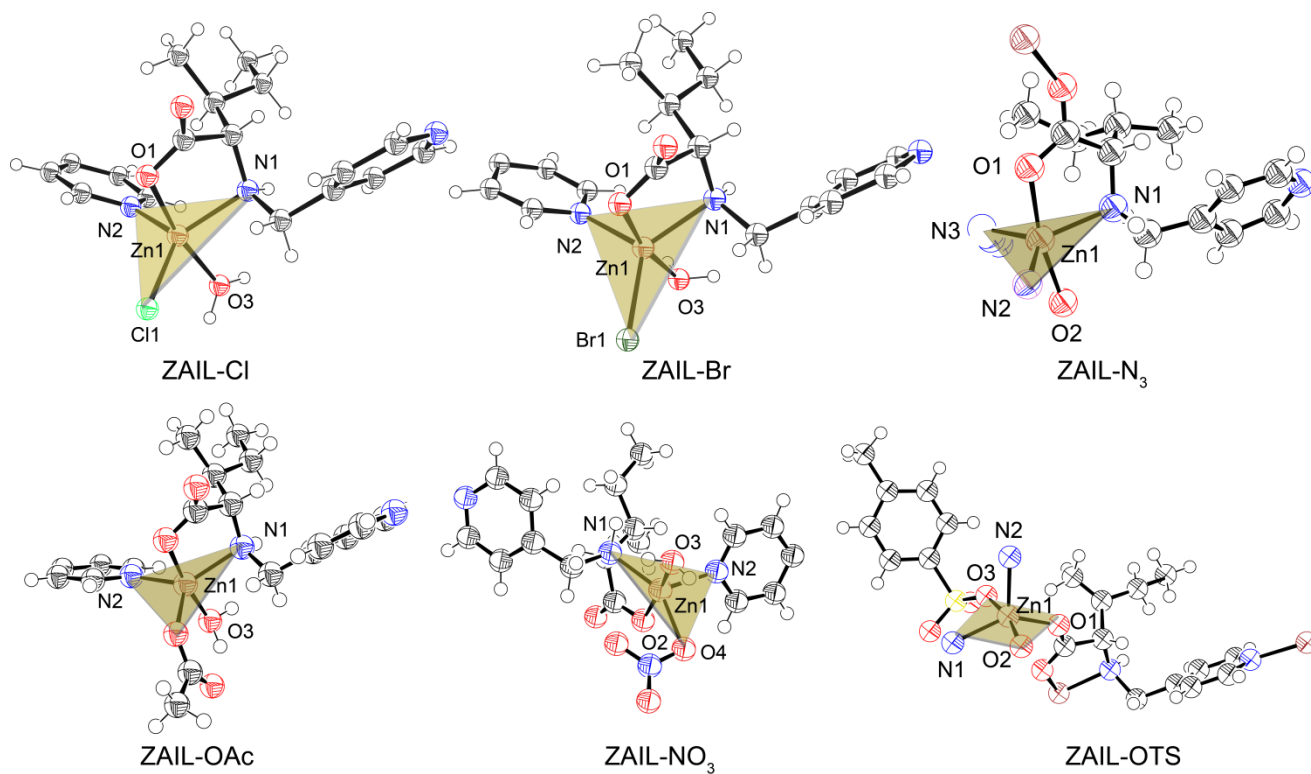


**Fig. S13** Molecular structure of the as-synthesized MOFs.

**Table S3.** Selected bond distances (Å) and geometry index values for all six MOFs.

	Zn-NH <sub>amine</sub>	Zn-N <sup>pyridine</sup>	Zn-X	Zn-O <sub>carboxylate</sub>	Zn-O <sub>water/carboxylate</sub>	geometry index ( $\tau$ )
ZAIL-Cl	2.093(4)	2.056(3)	2.2252(14)	2.160(4)	2.136(4)	0.725
ZAIL-Br	2.103(16)	2.061(16)	2.732(3)	2.169(14)	2.142(13)	0.721
ZAIL-OAc	2.109(5)	2.050(5)	1.963(5)	2.115(6)	2.097(5)	0.657
ZAIL-NO <sub>3</sub>	2.094(10)	2.071(11)	2.243	2.107(8)	2.085(8)	0.851
ZAIL-N <sub>3</sub>	2.084(10)	2.030(12)	1.972(15)	2.138(10)	2.098(12)	0.705
ZAIL-OTs	2.102(5)	2.089(5)	2.154(4)	2.070(4)	1.962(4)	0.421

**Table S4.** Hydrogen bonding parameters for all ZAIL-Cl, ZAIL-Br, ZAIL-OAc, and ZAIL-NO<sub>3</sub>.

	D-H...A (Å)	D...A (Å)	>D-H...A (°)
ZAIL-Cl			
C3-H3...O2 <sup>[a]</sup>	3.106(1)	2.973(1)	90.90(1)
C9-H9...O1 <sup>[b]</sup>	3.335(1)	2.475(1)	133.83(1)
C5-H5B...O1 <sup>[b]</sup>	3.425(1)	2.499(1)	159.68(1)
O3-H3B...O1 <sup>[c]</sup>	3.311(1)	2.675(1)	126.92(1)
N1-H1...O1 <sup>[b]</sup>	2.933(1)	2.036(1)	167.57(1)
ZAIL-Br			
O3-H3B...O1 <sup>[d]</sup>	2.582(1)	2.301(1)	98.48(1)
O3-H3A...O1 <sup>[d]</sup>	2.582(1)	2.069(1)	116.26(1)
N1-H1...O2 <sup>[e]</sup>	2.926(1)	1.968(1)	165.33(1)
C12-H12...O2 <sup>[d]</sup>	3.343(1)	2.484(1)	153.71(1)
C5-H5B...O2 <sup>[d]</sup>	3.440(1)	2.481(1)	169.82(1)
ZAIL-OAc			
O3-H3A...O2 <sup>[b]</sup>	2.680(6)	1.780(4)	154.09(3)
N1-H1...O1 <sup>[b]</sup>	2.887(6)	2.027(4)	157.28(3)
C5-H5A...O1 <sup>[b]</sup>	3.438(8)	2.483(4)	167.85(4)
C12-H12...O1 <sup>[b]</sup>	3.333(7)	2.500(1)	149.25(4)
ZAIL-NO <sub>3</sub>			
C5-H5A...O10 <sup>[a]</sup>	3.544(1)	2.674(1)	149.51(1)
N1-H1...O1 <sup>[d]</sup>	2.824(1)	1.889(1)	158.46(1)
O8-H8...O10 <sup>[a]</sup>	3.313(1)	2.943(1)	94.82(1)
C5-H5B...O1 <sup>[d]</sup>	3.471(1)	2.579(1)	153.69(1)
C9-H9...O1 <sup>[f]</sup>	3.305(1)	2.457(1)	151.56(1)

**Symmetry operations:** <sup>[a]</sup> x, y, z; <sup>[b]</sup> x+1, y, z; <sup>[c]</sup> -x+1/2+1, -y+1, z+1/2; <sup>[d]</sup> x-1, y, z; <sup>[e]</sup> -x+1/2, -y-1, z-1/2; <sup>[f]</sup> -x+1, y+1/2, -z+1.

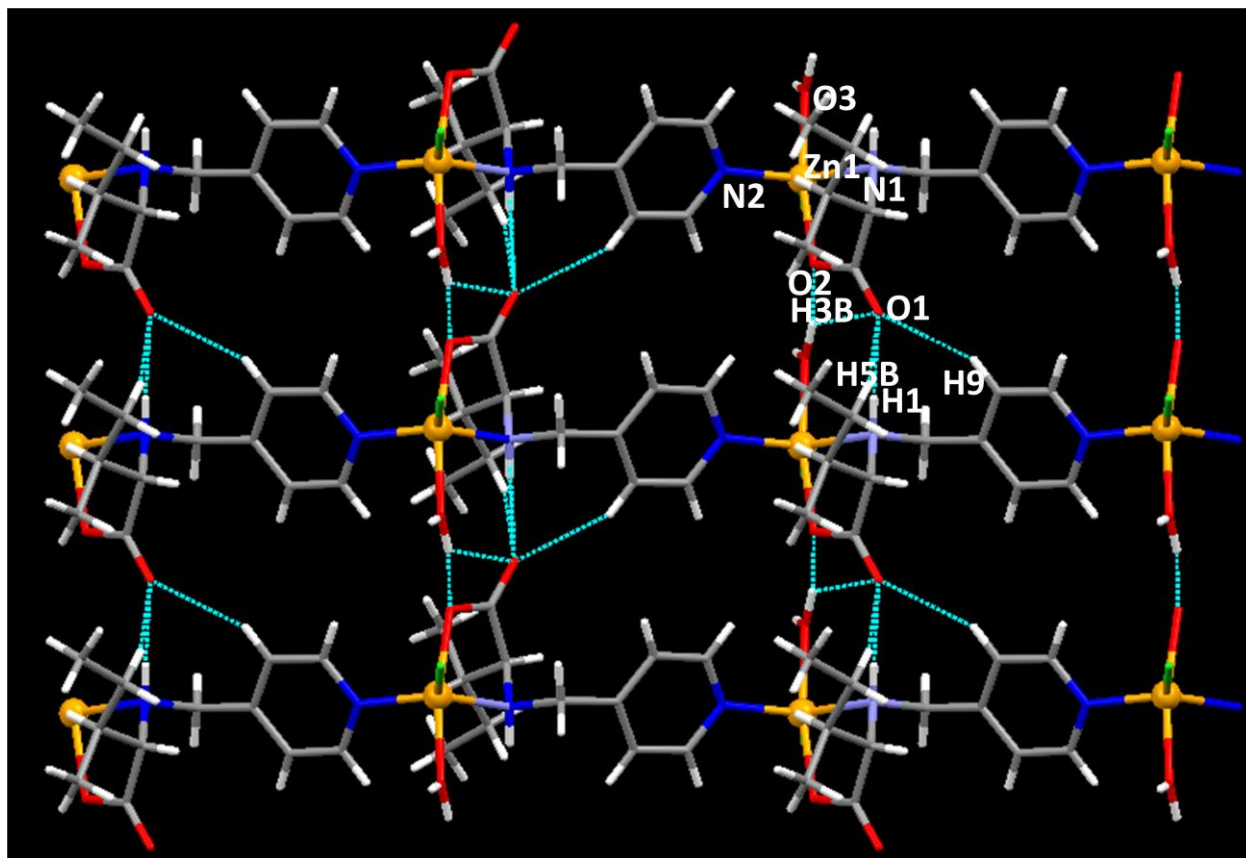


**Fig. S14** View of 2D arrangement via C-H...O and N-H...O weak interactions for ZAIL-Cl (view along b-axis).

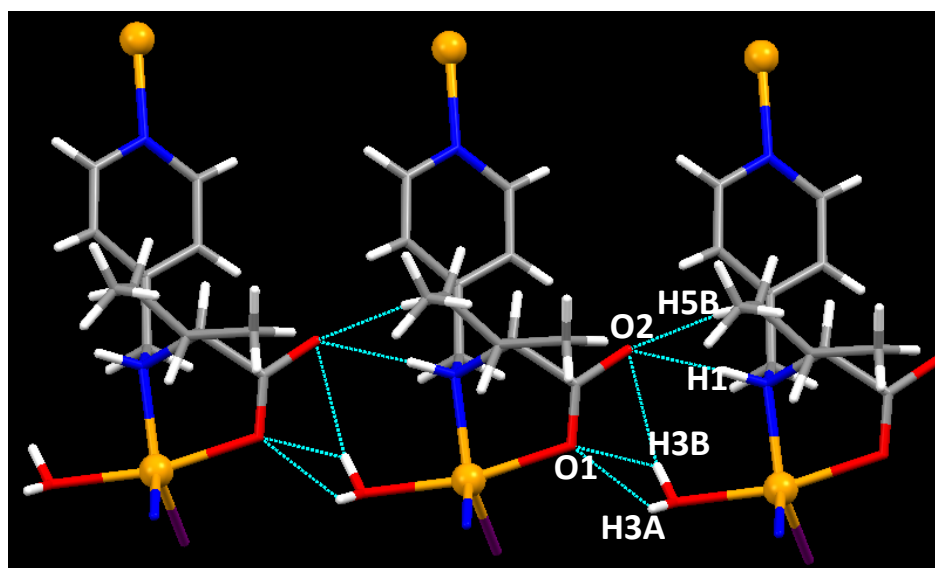


**Fig. S15** View of 2D chain arrangement via C-H...O and N-H...O weak interactions for ZAIL-Br (view along b-axis).

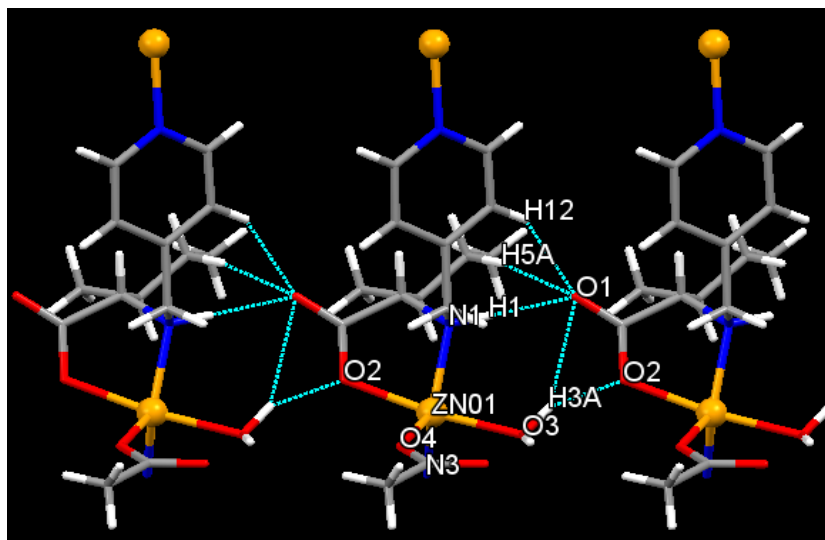


**Fig. S16** View of 2D chain arrangement via C–H...O and N–H...O weak interactions for ZAIL-OAc (view along b-axis).

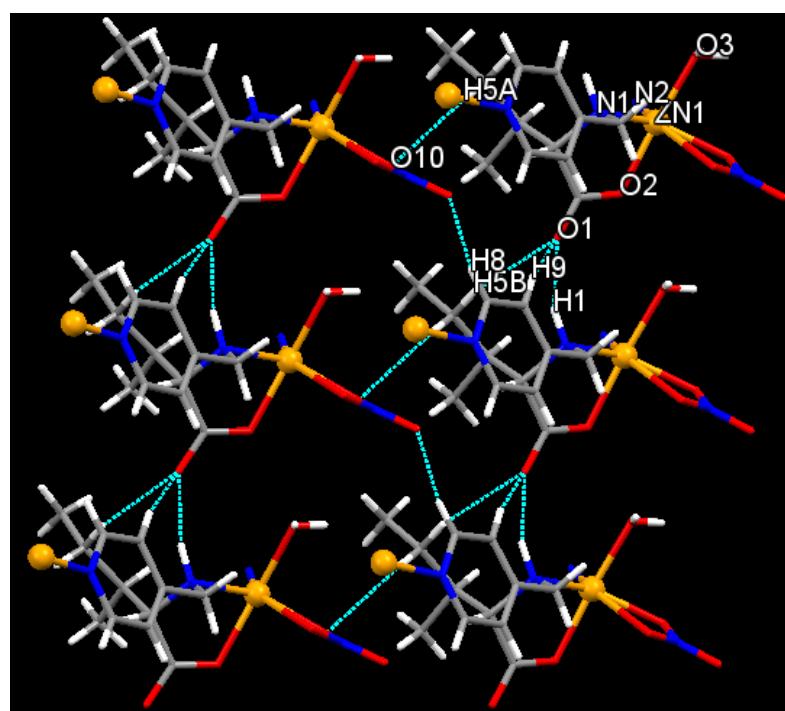


**Fig. S17** View of 2D arrangement via C–H...O and N–H...O weak interactions for ZAIL-NO<sub>3</sub> (view along b-axis).

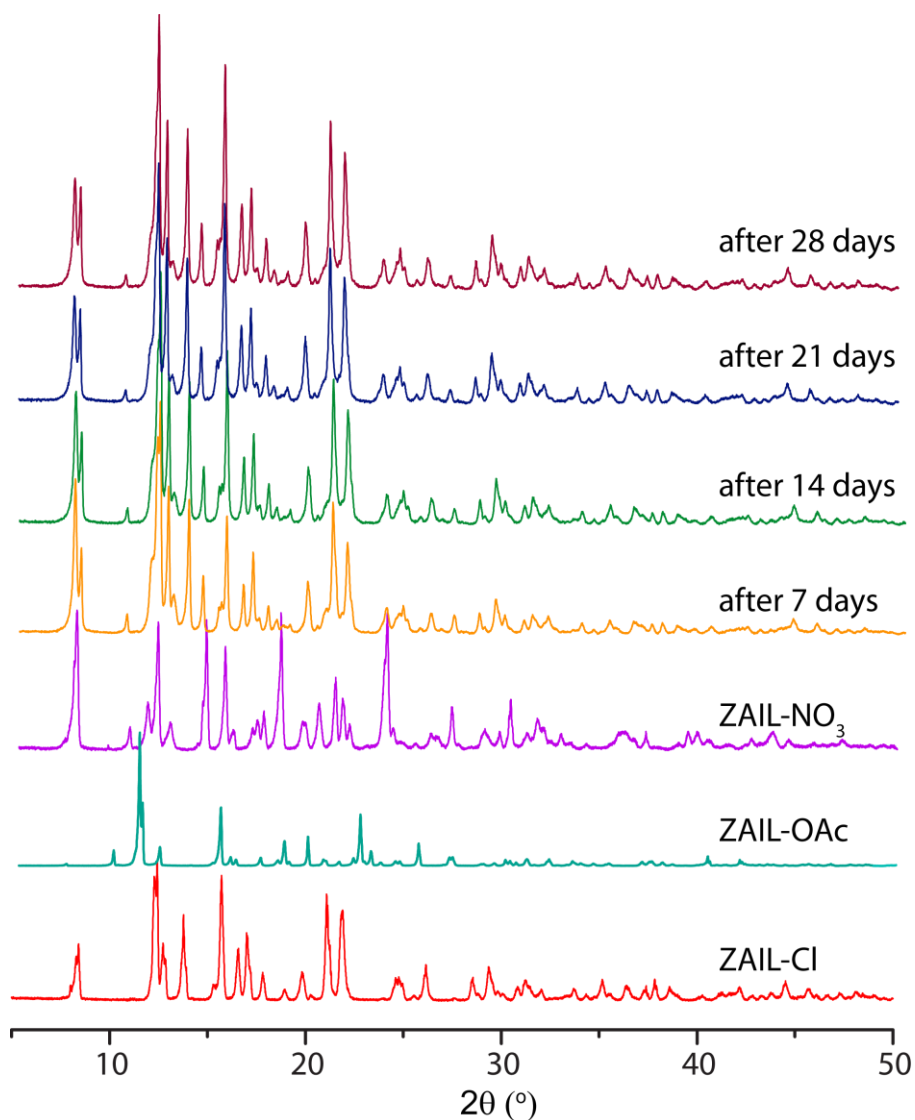


**Fig. S18** Time dependent PXRD spectra displaying preferential uptake of ZAIL-OAc for particular ion at room temperature.

**Table S5.** Preferential uptake of particular ion from a mixture of ions during MOF formation.

Sample	Gel	Mixture of ions	RT	60 °C
1.	ZAIL gel	Cl <sup>-</sup> and Br <sup>-</sup>	ZAIL-Br	ZAIL-Br
2.	ZAIL gel	Cl <sup>-</sup> and NO <sub>3</sub> <sup>-</sup>	*ZAIL- NO <sub>3</sub>	*ZAIL- NO <sub>3</sub>
3.	ZAIL gel	Cl <sup>-</sup> and OAc <sup>-</sup>	ZAIL-Cl	ZAIL-Cl
4.	ZAIL gel	Cl <sup>-</sup> and N <sub>3</sub> <sup>-</sup>	ZAIL- N <sub>3</sub>	ZAIL- N <sub>3</sub>
5.	ZAIL gel	Cl <sup>-</sup> , OAc <sup>-</sup> and NO <sub>3</sub> <sup>-</sup>	ZAIL- NO <sub>3</sub>	ZAIL- NO <sub>3</sub>
6.	ZAIL gel	Cl <sup>-</sup> and OTs <sup>-</sup>	ZAIL-Cl	ZAIL-Cl

\* It contains minor amount of ZAIL-Cl determined from PXRD pattern.

## 7. Computational Details

All the calculations have been carried out with Turbomole 7.0 [1,2] using the TZVP basis set (3) and the PBE [4] functional. Dispersion corrections [5] have been included in all the geometry optimization calculations. The resolution of identity (RI) [6] along with the multipole accelerated RI (marij) [7] approximations have been used for an accurate and efficient treatment of the electronic Coulomb term in the DFT calculations. Solvent corrections have also been included in all the calculations using the cosmo model [8], with epsilon ( $\epsilon$ ) = 80.1, to model the water (H<sub>2</sub>O) as a solvent, which has been employed to study the reaction involved.

The optimized geometries of the structures reported in the manuscript (the atomic symbol followed by the three Cartesian coordinates, in Å).

### a) Ligand (IL):

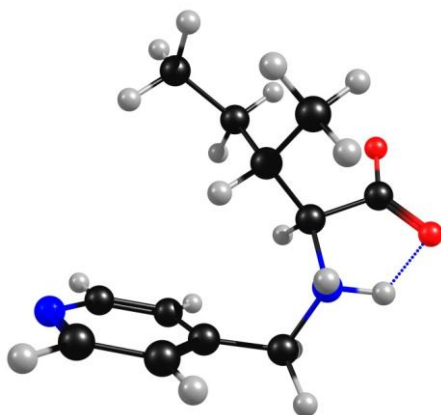


**Fig. S19** Optimized structure of the ligand IL.

The color scheme is as follows: carbon: black, oxygen: red, nitrogen: blue, hydrogen: grey, chloride ion: green. The interaction is being shown by the fragmented bond (blue).

C	1.785066	-0.559272	-9.479057
H	2.384794	0.331644	-9.685002
C	0.475360	-0.429068	-9.009844
H	0.050356	0.562643	-8.843597
C	-0.273474	-1.585261	-8.764275
C	0.341286	-2.824423	-8.986437

H	-0.191038	-3.760358	-8.802341
C	1.656002	-2.851355	-9.454427
H	2.154394	-3.807429	-9.635648
C	-1.715023	-1.509654	-8.333879
H	-1.950994	-2.276360	-7.585590
H	-1.962620	-0.523959	-7.921993
C	-2.597795	-0.712952	-10.606456
H	-2.090891	0.173305	-10.197573
C	-4.095508	-0.317231	-10.847188
C	-1.819499	-1.227332	-11.833961
H	-0.901063	-1.696498	-11.435530
C	-1.360479	-0.055401	-12.720986
H	-2.242709	0.394404	-13.200530
H	-0.931476	0.724971	-12.068676
C	-0.316259	-0.453086	-13.767633
H	0.019592	0.428811	-14.332566
H	-0.712821	-1.177951	-14.493904
H	0.569677	-0.904106	-13.292249
C	-2.605397	-2.295884	-12.604281
H	-2.932302	-3.122687	-11.953268
H	-1.988149	-2.742538	-13.395189
H	-3.501031	-1.857920	-13.069109
N	2.380143	-1.744349	-9.707758
N	-2.636738	-1.739833	-9.496845
H	-3.670850	-1.683481	-9.227999
H	-2.487659	-2.683616	-9.880033
O	-4.923112	-0.854010	-10.037164
O	-4.338408	0.488911	-11.771355

**b) Monomeric structure of ZAIL-Cl MOF:**

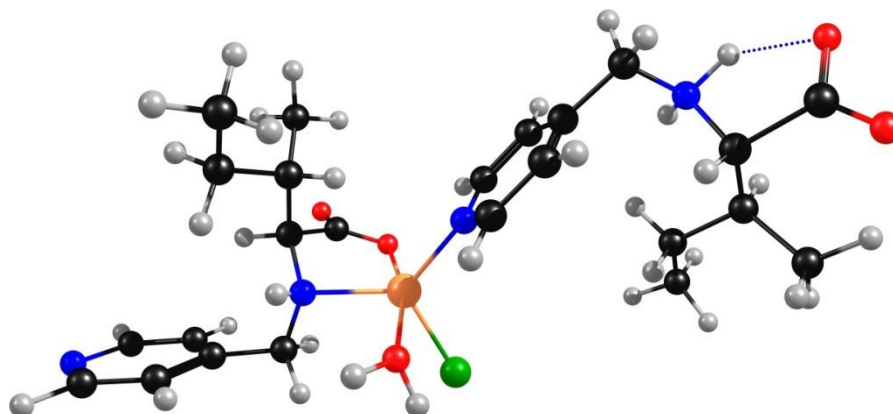


**Fig. S20** Optimized structure of ZAIL-Cl monomeric unit

The color scheme is as follows: carbon: black, oxygen: red, nitrogen: blue, hydrogen: grey, chloride ion: green, Zn: orange. The interaction is being shown by the fragmented bond (blue).

N	2.785693	8.011494	7.420372
C	2.082665	6.975559	7.932201
C	2.180843	5.688766	7.417530
C	3.029992	5.446327	6.329699
C	3.728162	6.529516	5.785259
C	3.588619	7.790546	6.357924
C	3.223878	4.045062	5.813884
N	4.177994	3.276963	6.684887
C	5.638874	3.656350	6.583335
C	6.267500	3.742309	7.993872
C	5.652040	4.921499	8.778932
C	6.058667	4.983884	10.252872
Zn	2.657282	9.823368	8.423179
Cl	4.271191	10.096832	10.001576
N	1.451865	11.453267	7.839011
C	1.707171	12.601805	8.760535
C	0.886535	13.822491	8.424910
C	1.183862	14.596534	7.294801
C	0.374249	15.690971	6.989149
N	-0.692436	16.058075	7.725279
C	-0.968482	15.313156	8.810962
C	-0.218098	14.199555	9.196851

C	0.057192	10.934233	7.874844
C	-0.198339	10.107275	6.589139
C	-0.306823	11.030084	5.355842
C	-0.050199	10.309086	4.030351
C	-0.103544	10.076430	9.155623
O	0.930544	9.378417	9.498622
O	-1.194279	10.084353	9.753400
C	-1.425911	9.199425	6.713969
O	4.270959	10.738308	6.925114
C	6.245114	2.547384	5.653340
O	5.525650	1.493908	5.561390
O	7.336396	2.783703	5.096077
C	7.794242	3.857306	7.925244
H	-1.293896	8.441972	7.498846
H	-2.324288	9.786819	6.956910
H	-1.607380	8.671231	5.767962
H	-1.308298	11.491813	5.354279
H	0.402912	11.873238	5.433192
H	-0.138896	11.002634	3.181790
H	0.963975	9.879307	4.008082
H	-0.764861	9.489626	3.865510
H	2.781201	12.827864	8.701071
H	1.498540	12.260316	9.784076
H	2.041503	14.362879	6.659129
H	0.592940	16.309240	6.113865
H	-0.495614	13.634899	10.089511
H	1.671818	11.754922	6.883700
H	-0.671093	11.759376	7.923809
H	0.688425	9.458946	6.453376
H	8.244684	2.999700	7.412190
H	8.091342	4.769078	7.383885
H	8.214586	3.909313	8.938476
H	5.930347	5.860876	8.269787
H	4.550785	4.873496	8.738432
H	5.523224	5.797700	10.763209
H	5.813727	4.042900	10.769720
H	7.134928	5.167966	10.377911
H	2.277550	3.490422	5.813754
H	3.637993	4.038552	4.798623
H	1.597909	4.885993	7.871597

H	1.434106	7.210174	8.777150
H	4.135637	8.656251	5.985565
H	4.384982	6.403980	4.923939
H	3.848139	3.272374	7.658577
H	5.722615	4.630676	6.083571
H	6.016985	2.801501	8.520648
H	-1.835749	15.621916	9.401590
H	4.982806	10.992325	7.542125
H	4.274048	11.418444	6.228540
H	4.252470	2.261982	6.336682

c) Monomeric structure of ZAIL-NO<sub>3</sub> MOF:

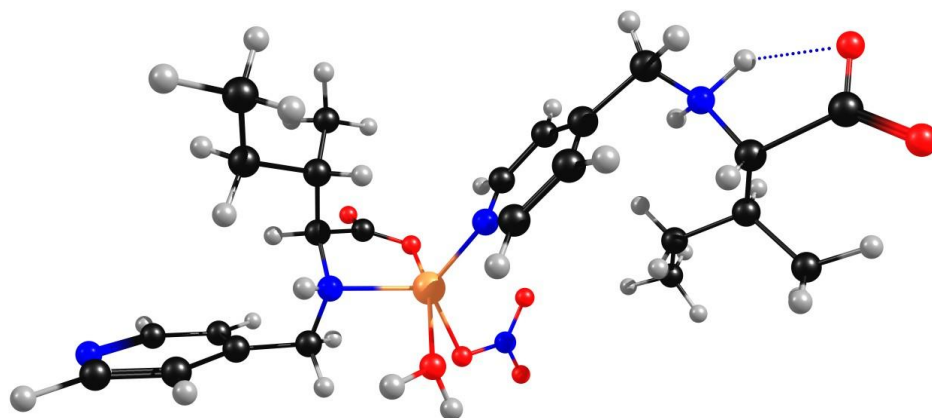


**Fig. S21** Optimized structure of ZAIL-NO<sub>3</sub> monomeric unit

The color scheme is as follows: carbon: black, oxygen: red, nitrogen: blue, hydrogen: grey, Zn: orange. The interaction is being shown by the fragmented bond (blue).

H	8.225781	5.746874	16.766178
N	6.774726	5.438743	15.314506
C	7.811937	5.019590	16.061739
H	5.418375	4.909504	13.833612
C	6.255705	4.554260	14.441025
H	6.269675	2.589658	13.549445
C	6.732543	3.252364	14.284751
C	7.808668	2.821017	15.072283
C	8.357868	3.735832	15.977957
H	9.200097	3.456782	16.614574
H	9.285695	1.297472	15.473751

C	8.311913	1.401372	14.975567
H	8.442789	1.110385	13.923527
N	7.377330	0.409633	15.592615
H	6.468828	0.495621	15.123552
H	7.120985	1.661986	17.315155
C	7.179602	0.592554	17.058641
C	8.405543	-0.004165	17.793837
O	8.810687	0.545930	18.832459
O	8.911963	-1.076182	17.272910
Zn	8.179006	-1.539497	15.399098
O	7.433239	-1.565317	13.255604
H	6.788015	-0.977670	12.824638
H	8.193017	-1.612978	12.646826
O	9.955590	-1.661059	14.395883
N	10.697564	-2.690533	14.765446
O	10.228948	-3.496208	15.595006
O	11.824717	-2.798176	14.257579
C	5.855714	-0.095806	17.476944
H	5.834777	-1.077059	16.966003
C	4.642019	0.722354	16.987662
H	4.829746	1.128913	15.978075
H	4.529441	1.601372	17.644628
H	5.902697	0.585842	19.547311
C	5.785129	-0.352845	18.985721
H	6.569397	-1.046830	19.318320
C	3.339105	-0.079133	16.943462
H	4.815286	-0.793733	19.254026
H	3.431999	-0.942425	16.265515
H	2.508517	0.543613	16.581326
H	3.058257	-0.461257	17.935703
N	7.071886	-3.208880	15.862616
C	7.313541	-3.786072	17.060544
H	8.024125	-3.267800	17.704822
C	6.189889	-3.789579	15.023720
H	6.029017	-3.287265	14.070203
C	5.544751	-4.981666	15.339263
H	4.843240	-5.415040	14.625622
C	5.822703	-5.609080	16.557905
C	6.708588	-4.976541	17.440478
H	6.944269	-5.409267	18.414027

C	5.263673	-6.966449	16.889793
H	4.376992	-7.202592	16.288651
H	5.001251	-7.039826	17.952326
N	6.282124	-8.037941	16.615712
H	5.895557	-8.996920	16.913804
H	7.147554	-7.849783	17.138031
C	6.555930	-8.349621	15.160317
C	5.735646	-9.663200	14.905379
O	5.475707	-9.971400	13.724174
O	5.405657	-10.287462	15.971669
H	6.143126	-7.543599	14.538518
C	8.077355	-8.467016	14.908981
H	8.476434	-9.185443	15.650141
C	8.763904	-7.101031	15.130062
H	8.476268	-6.680741	16.108364
H	8.378963	-6.392231	14.376248
C	10.292499	-7.136979	15.078559
H	10.695433	-7.851410	15.813274
H	10.698241	-6.141271	15.309767
H	10.665809	-7.426096	14.086071
C	8.372530	-9.011330	13.506967
H	7.921710	-9.997936	13.348944
H	9.456644	-9.101133	13.358257
H	7.977010	-8.331506	12.736113

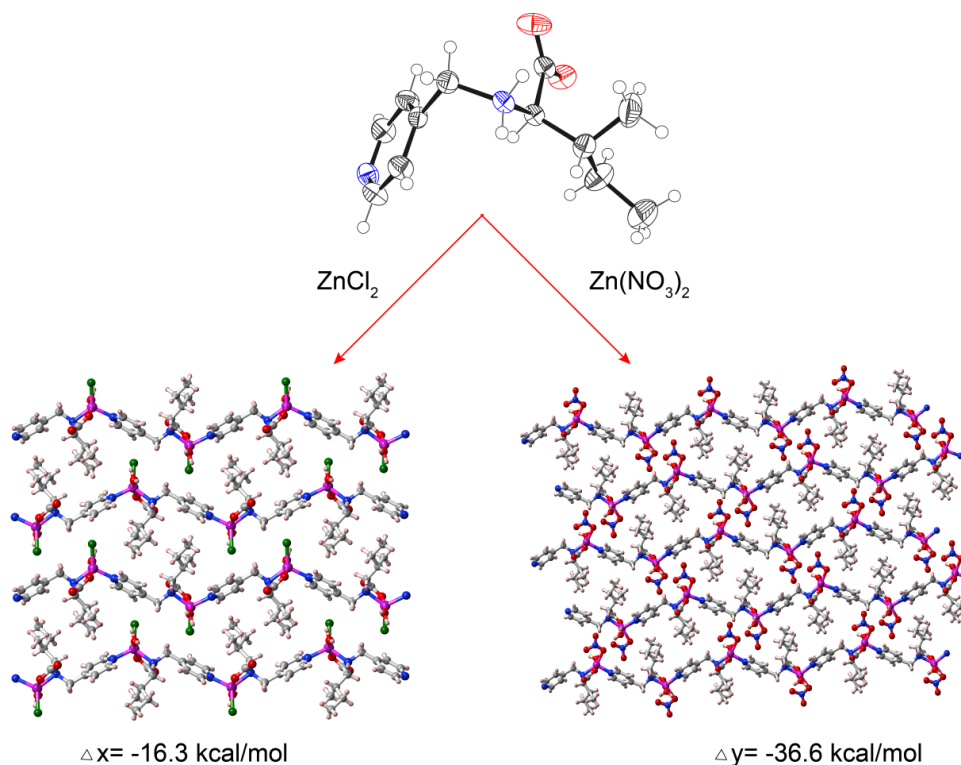


**Fig. S22** Stabilization of ZAIL-NO<sub>3</sub> MOF monomer as compared to that of the ZAIL-Cl MOF monomer

## 8. References

1. S. Saha, J. Bachl, T. Kundu, D. D. Díaz and R. Banerjee, *Chem. Commun.*, 2014, **50**, 3004.
2. *CrysAlisPro*, v. 1.171.33.49b, Oxford Diffraction Ltd., Abingdon, UK, 2009.
3. A. Altomare, G. Casciarano, C. Giacovazzo and A. Guagliardi, *J. Appl. Crystallogr.* 1993, **26**, 343.
4. G. M. Sheldrick, *Acta Crystallogr., Sect. A*, 2008, **64**, 112.
5. L. J. Farrugia, *WinGx*, v. 2014.1, *An Integrated System of Windows Programs for the Solution, Refinement and Analysis of Single-Crystal X-ray Diffraction Data*, Department of Chemistry, University of Glasgow, Glasgow, 2014.